64-12

BSD-TDR-64-37

437525

Derivation of the Guidance Equations for the USAF ATHENA

30 MARCH 1964

Prepared by L. K. HERMAN, R. M. ALLMAN, and B. KATZ
Guidance and Control Subdivision

Prepared for COMMANDER
BALLISTIC SYSTEMS DIVISION
AIR FORCE SYSTEMS COMMAND
UNITED STATES AIR FORCE
Norton Air Force Base, California

ELECTRONICS DIVISION • AEROSPACE CORPORATION
CONTRACT NO. AF 04(695)-269

BSD-TDR-64-37

Report No.
TDR-269(4810-31)-1

DERIVATION OF THE GUIDANCE EQUATIONS FOR THE USAF ATHENA

Prepared by
L. K. Herman,
R. M. Allman, and
B. Katz
Guidance and Control Subdivision

AEROSPACE CORPORATION
El Segundo, California

Contract No. AF 04(695)-269

30 March 1964

Prepared for
COMMANDER BALLISTIC SYSTEMS DIVISION
Air Force Systems Command
United States Air Force
Norton Air Force Base, California

DERIVATION OF THE GUIDANCE EQUATIONS FOR THE USAF ATHENA

Prepared by:

Louis K. Herman
L. K. Herman
Control Systems Department

Richard M Allman
R. M. Allman
Control Systems Department

Bernard Katz
B. Katz
Guidance Systems Department

This technical documentary report has been reviewed and approved by:

A. J. Schiewe
A. J. Schiewe, Department Head
Control Systems Department

K. F. Steffan
K. F. Steffan,
Associate Department Head
Guidance Systems Department

E. A. Goldberg
E. A. Goldberg, Associate Director
Guidance and Control Subdivision

Arthur Gelernter
Arthur Gelernter, Manager
Guidance and Performance
ATHENA Program

For Ballistics Systems Division
Air Force Systems Command

Capt. David W. Clonts
Capt. D. W. Clonts, BSYA

ABSTRACT

The USAF ATHENA is a re-entry test vehicle which has four solid propellant stages. A midcourse correction type of guidance is used to compensate for boost dispersions by adjusting the third stage attitude and ignition time. The guidance computations are performed in a ground based digital computer using radar data obtained after second stage burnout. Because this is a re-entry test vehicle, the guidance system must cause the payload to meet various re-entry constraints as well as the usual impact point constraint. The complete derivation of the guidance equations and a description of the entire guidance loop are presented in this report.

CONTENTS

FIGURES

SECTION 1

INTRODUCTION

The purpose of the USAF ATHENA vehicle is to deliver test payloads at typical ballistic missile re-entry conditions for the Advanced Ballastic Re-Entry Systems (ABRES) program. The ATHENA is launched from Green River, Utah, and the payloads impact on the White Sands Missile Range (WSMR) in New Mexico.

The ATHENA vehicle, consisting of four solid propellant stages which are burned to propellant depletion, is launched from a rail launcher. The launcher is oriented so as to compensate for winds, based on meteorological data obtained just prior to launch. The first and second stages are fired in an upward direction and are controlled by a combination of spin stabilization and fixed aerodynamic fins. This type of control, which causes the vehicle to fly near zero angle of attack, has been used on many sounding rockets. After second stage burnout the vehicle is despun and a reaction jet attitude control system orients the third and fourth stages in a nominal attitude relative to a prelaunch-erected gyro reference system.

The attitude corrections and third stage ignition time required to compensate for dispersions which occur during first and second stage operation are computed using radar data acquired after second stage burnout. These computations are performed in a ground based digital computer at WSMR and the necessary commands are then transmitted to the vehicle. After the vehicle has stabilized in the proper attitude, it is spun up to a rate high enough to inertially stabilize the third and fourth stages during thrusting, after which the attitude control system is separated. The third stage is then ignited at the computed time and the fourth stage ignites at a predetermined time after third stage burnout.

The purpose of this document is to present the derivation of the equations used to determine the required third and fourth stage attitude and ignition time from the radar data acquired after second stage burnout.

SECTION 2

PROBLEM STATEMENT

The ATHENA guidance problem is similar to the classical midcourse correction problem; that is, the position and velocity of the vehicle are determined with the use of ground based radars and this information is then used to determine the direction and time of initiation of a velocity increment that satisfies given constraints. The magnitude of the velocity increment cannot be varied in this case since the solid propellant stages are burned to fuel depletion. The direction of the velocity increment is controlled by vehicle orientation and fixed by spin-stabilizing the third and fourth stages after orientation.

Position and velocity for the guidance computation need be determined at only one instant of time, and for simplification this is chosen as nominal third stage ignition time for all flights. The time of flight at which actual radar data becomes available varies from flight to flight, but it is always acquired after the vehicle has left the sensible atmosphere. Hence, a form of Kepler's equations may be used for predicting position and velocity at the predetermined time from position and velocity derived from the radar data at any exo-atmospheric read-out time (Reference 1).

In addition to constraining the impact point, the corrections which are computed by these equations must constrain the vehicle to an angle of attack as near null as possible at a predetermined altitude in order to satisfy test requirements. However, if the launch dispersions require corrections that would reduce the re-entry separation distance between the payload and the fourth stage below a critical minimum, it is necessary to substitute a separation distance constraint for the angle of attack constraint. The method used to obtain the solution to the guidance problem is discussed in the next section.

SECTION 3

METHOD OF SOLUTION

The analytical description of the problem is derived from two basic sets of information. These are (1) the classical equations of motion and (2) the equations which analytically express the desired program constraints.

The equations of motion are written in vector form in an earth-centered inertial coordinate system and are integrated to obtain the dynamics equations. The variables in these equations are the body attitude (expressed in direction cosines), the third stage ignition time (expressed in terms of the fourth stage burnout time), the time and position at the test altitude and impact, and the velocity at the test altitude. The dynamics equations comprise a set of nine nonlinear equations with fifteen unknowns.

Six constraint equations express the desired impact point and either the angle of attack constraint or separation distance constraint in terms of the variables in the equations of motion. This results in a total set of fifteen equations with fifteen unknowns. The simultaneous solution of these nonlinear equations yields the required attitude and ignition time of the third stage.

A linear solution of these equations, made possible by expanding the nonlinear terms in a Taylor series or equivalent technique and retaining only first order terms, will not result in a solution which is sufficiently accurate over the required range of inputs. The significant part of the inaccuracy in this solution is a result of the linearization of terms involving products of two variables. Because all of these terms are functions of the body attitude, which is determined in the solution, it is possible to recompute the "nominal" values in the linear approximations for these terms after completing the solution of the linearized equations. This leads to an iteration procedure which converges on a solution which is sufficiently close to the solution obtained from a complete trajectory integration program to meet all of the ATHENA requirements.

The solution therefore consists of the following steps.

a. Integrate the differential equations of motion to obtain nonlinear dynamics equations.

b. Write algebraic equations which analytically describe the system constraints.

c. Linearize these equations, where necessary, using a Taylor series expansion or equivalent technique and retain only nominal and first order terms.

d. Solve the linearized equations for the unknown variables, which include the direction cosines of the body axis and the third stage ignition time.

e. Recompute the "nominal" terms which are functions of body attitude in the Taylor series approximation.

f. Repeat steps d and e until the body attitude does not change.

The derivation of these equations is described in detail in the remainder of this report. The solution has been programmed on a digital computer and is presently part of the real-time computer program that is used in the guidance and command of the ATHENA vehicle.

SECTION 4

THE DERIVATION

4.1 DYNAMICS EQUATIONS

The dynamics equations are derived in vector form starting with Newton's law,

$$\underline{F} = m\ddot{\underline{D}} \tag{1}$$

Figure 1 is a geometric description of the problem.

The acceleration of the vehicle results from gravitational and thrust forces, therefore

$$\underline{F} = m(\underline{a} + \underline{g}) \tag{2}$$

and

$$\ddot{\underline{D}} = \underline{a} + \underline{g} \tag{3}$$

Integrating both sides of Equation (3) from t_R to t (Figure 2 is a description of the time notation) where $t > t_\tau$ and rearranging yields

$$\dot{\underline{D}} = \dot{\underline{D}}_R + \int_{t_0}^{t_\tau} \underline{a}\, dt + \int_{t_R}^{t} \underline{g}\, dt \tag{4}$$

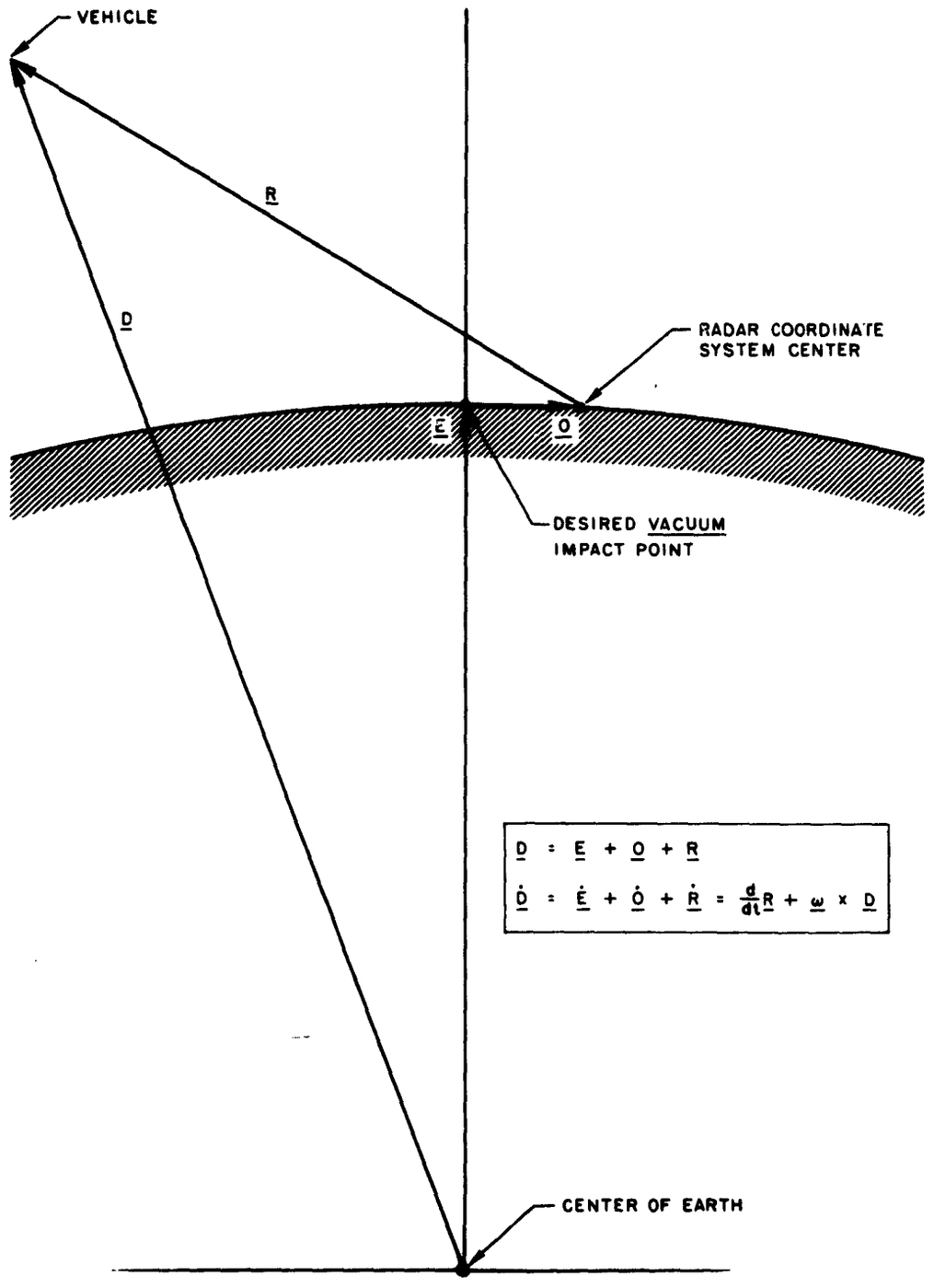

Figure 1. Geometric Description

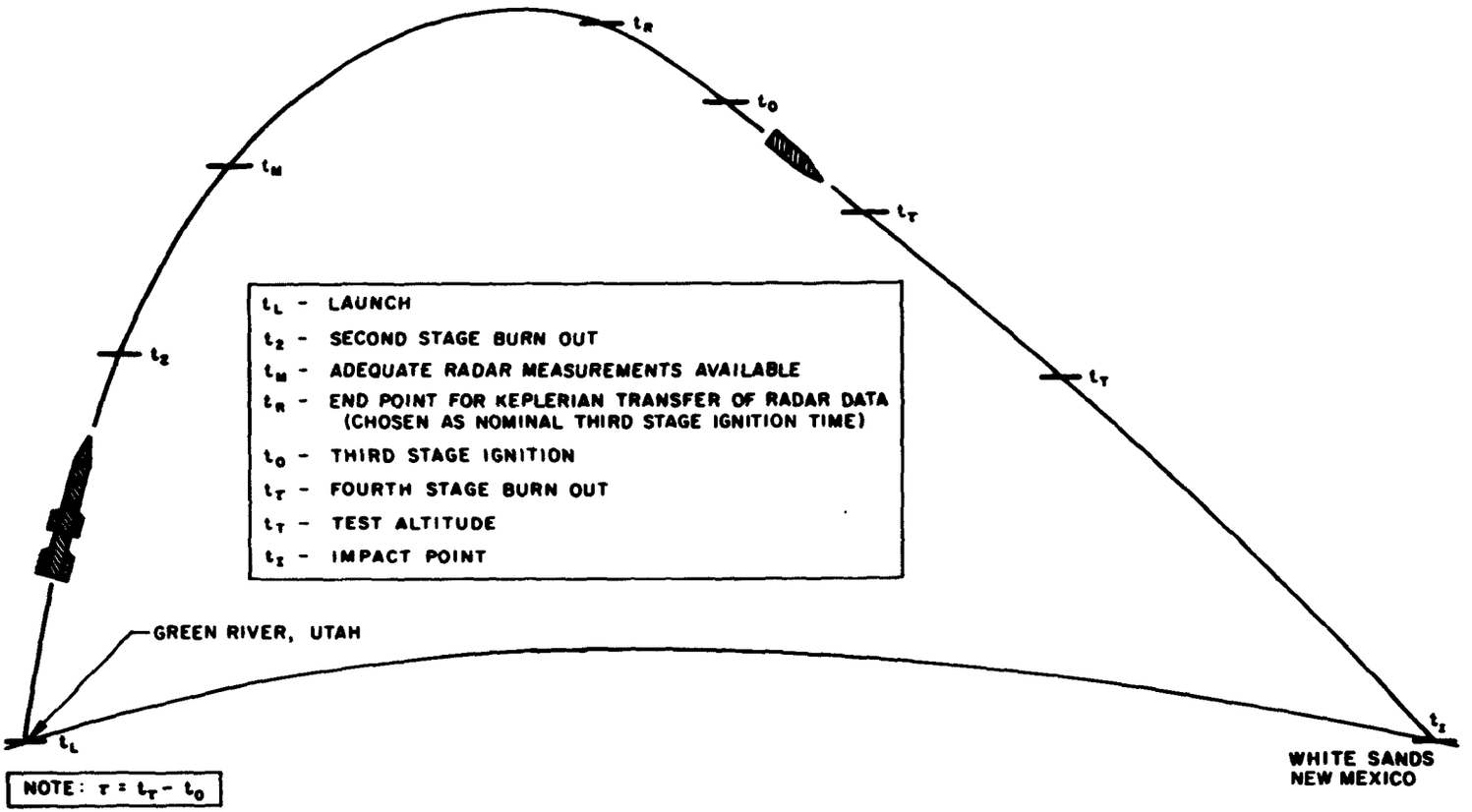

Figure 2. Time Notation Description

Integrating both sides of Equation (4) from t_R to t where $t > t_\tau$ and rearranging terms gives

$$\underline{D} = \underline{D}_R + \dot{\underline{D}}_R(t - t_R) + \int_{t_0}^{t_\tau}\int_{t_0}^{t_1} \underline{a}\, dt\, dt_1 + (t - t_\tau)\int_{t_0}^{t_\tau} \underline{a}\, dt$$

$$+\int_{t_R}^{t}\int_{t_R}^{t_1} \underline{g}\, dt\, dt_1 \qquad (5)$$

The velocity increment due to the third and fourth stage thrusting is

$$\underline{\Delta V} \triangleq \int_{t_0}^{t_\tau} \underline{a}\, dt \qquad (6)$$

The distance traveled during third and fourth stage thrusting due only to the vehicle propulsion system is

$$\underline{\Delta D} \triangleq \int_{t_0}^{t_\tau}\int_{t_0}^{t_1} \underline{a}\, dt\, dt_1 \qquad (7)$$

At the time the vehicle reaches the test altitude, $t = t_T$ and Equation (5) becomes

$$\underline{D}_T = \underline{D}_R + \dot{\underline{D}}_R(t_T - t_R) + \underline{\Delta D} + \underline{\Delta V}(t_T - t_\tau) + \int_{t_R}^{t_T}\int_{t_R}^{t_1} \underline{g}\, dt\, dt_1 \qquad (8)$$

At the time the vehicle reaches the impact point, $t = t_I$ and Equation (5) becomes

$$\underline{D}_I = \underline{D}_R + \dot{\underline{D}}_R(t_I - t_R) + \underline{\Delta D} + \underline{\Delta V}(t_I - t_\tau) + \int_{t_R}^{t_I}\int_{t_R}^{t_1} \underline{g}\ dt\ dt_1 \tag{9}$$

An equation which relates the velocity at the test altitude to the other problem variables is required because of the angle of attack constraint. At the time the vehicle reaches the test altitude, $t = t_T$ and Equation (4) becomes

$$\dot{\underline{D}}_T = \dot{\underline{D}}_R + \underline{\Delta V} + \int_{t_R}^{t_T} \underline{g}\ dt \tag{10}$$

Since the air mass is assumed to rotate with the earth, the required velocity equation is

$$\frac{d}{dt}\underline{D}_T = \dot{\underline{D}}_T - \underline{\omega} \times \underline{D}_T \tag{11}$$

Substituting Equation (10) into Equation (11) gives

$$\frac{d}{dt}\underline{D}_T = \dot{\underline{D}}_R + \underline{\Delta V} + \int_{t_R}^{t_T} \underline{g}\ dt - \underline{\omega} \times \underline{D}_T \tag{12}$$

Equations (8), (9) and (12) represent the nine scalar equations that define the dynamics from t_R to t_I.

4.2 LINEARIZING THE DYNAMICS EQUATIONS

In Equations (8) and (9), terms of the form $(\underline{\Delta V})\,(t_i)$ where i = T, I, τ must be linearized because they are products of the unknown variables. The linearization in this case is performed in the following manner.

Let

$$\underline{\Delta V} = \underline{\Delta V}_N + \delta\underline{\Delta V} \tag{13}$$

and

$$t_T = t_{TN} + \delta t_T \tag{14}$$

therefore

$$(\underline{\Delta V})(t_T) = (\underline{\Delta V}_N + \delta\underline{\Delta V})(t_{TN} + \delta t_T) \tag{15}$$

Expanding and neglecting products of perturbations

$$(\underline{\Delta V})(t_T) \approx \underline{\Delta V}(t_{TN}) + \underline{\Delta V}_N(t_T) - \underline{\Delta V}_N(t_{TN}) \tag{16}$$

Similar expressions result for t_I and t_τ.

In Equations (8), (9) and (12) the terms involving $\underline{g}$ are linearized as follows.

$$\int_{t_R}^{t_T} \underline{g}\, dt \approx \int_{t_R}^{t_{TN}} \underline{g}\, dt - \underline{g}_{TN}(t_{TN} - t_T) \tag{17}$$

and

$$\int_{t_R}^{t_T}\int_{t_R}^{t_1} \underline{g}\, dt\, dt_1 \approx \int_{t_R}^{t_{TN}}\int_{t_R}^{t_1} \underline{g}\, dt\, dt_1 + (t_T - t_{TN})\int_{t_R}^{t_{TN}} \underline{g}\, dt \qquad (18)$$

A similar equation results for the double integral of $\underline{g}$ between t_R and t_I.

The linearized form of Equations (8), (9), and (12) is presented in the linearized equation summary.

Because the solid propellant engines are burned to fuel depletion, the magnitudes of $\underline{\Delta V}$ and $\underline{\Delta D}$ are constants which can be determined before flight. The spin stabilization of the third and fourth stages orients the vehicle in inertial space and as a result $\underline{\Delta V}$ and $\underline{\Delta D}$ are parallel and are completely defined by their magnitudes and the direction cosines of the body roll axis. That is, $\underline{\Delta D}$ can be expanded as a function of the body axis direction cosines as follows

$$\underline{\Delta D} = |\underline{\Delta D}|(DCx)\,\hat{i} + |\underline{\Delta D}|(DCy)\,\hat{j} + |\underline{\Delta D}|(DCz)\hat{k} \qquad (19)$$

The vectors $\underline{D}_R$ and $\underline{\dot{D}}_R$ can be determined from the radar data at the preselected time t_R. The vector $\underline{\omega}$ is the rotation rate of the earth and the terms involving $\underline{g}$ have been linearized as shown in Equations 17 and 18.

Only the three body axis direction cosines are unknown in the vectors $\underline{\Delta V}$ and $\underline{\Delta D}$. The other unknowns in Equations (8), (9), and (12) are: $\underline{D}_T$, three; t_T, one; t_τ, one; $\underline{D}_I$, three; t_I, one; and $\frac{d}{dt}\underline{D}_T$, three. The final count finds nine equations and fifteen unknowns. Therefore, six constraint equations must be written to complete the analytical description of the problem.

4.3 DIRECTION COSINE CONSTRAINT

The first of the six constraints relates the three body axis direction cosines of which only two are independent. The equation is

$$(DCx)^2 + (DCy)^2 + (DCz)^2 = 1 \tag{20}$$

To linearize Equation (20), let

$$DCx = DCx_N + \delta DCx \tag{21}$$

$$DCy = DCy_N + \delta DCy \tag{22}$$

$$DCz = DCz_N + \delta DCz \tag{23}$$

Substituting Equations (21), (22), and (23) into Equation (20), expanding, and neglecting products of perturbations, yields

$$(DCx)(DCx_N) + (DCy)(DCy_N) + (DCz)(DCz_N) \approx 1 \tag{24}$$

This is the linearized direction cosine constraint.

4.4 IMPACT POINT CONSTRAINT

The impact point constraint can be written from inspection of Figure 1. It is simply

$$\underline{D}_I = \underline{E}_I \tag{25}$$

Because the transformation between the earth fixed coordinate system and the inertial coordinate system is a function of the unknown time t_I, the exact values of the components of $\underline{E}_I$ are not known before flight in the inertial

coordinate system. To overcome this problem, the right hand side of Equation (25) is replaced by the first two terms of its Taylor series expansion

$$\underline{E}_I \approx \underline{E}_{IN} + \dot{\underline{E}}_{IN}(t_I - t_{IN}) \tag{26}$$

in addition

$$\dot{\underline{E}}_{IN} = \frac{d}{dt}\underline{E}_{IN} + \underline{\omega} \times \underline{E}_{IN} \tag{27}$$

Because the rate of change of $\underline{E}_{IN}$ in the earth fixed system is zero, Equation (27) becomes

$$\dot{\underline{E}}_{IN} = \underline{\omega} \times \underline{E}_{IN} \tag{28}$$

therefore

$$\underline{D}_I \approx \underline{E}_{IN} + \underline{\omega} \times \underline{E}_{IN}(t_I - t_{IN}) \tag{29}$$

Equation (29) is the linear form of the impact point constraint.

4.5 TEST ALTITUDE CONSTRAINT

The test altitude constraint defines the altitude at which the angle of attack or separation distance constraint applies. By inspection this constraint can be written as follows.

$$|\underline{D}_T| = |\underline{D}_{TN}| \tag{30}$$

Equation (30) must be linearized to allow a linear solution of the whole system of equations. This linearization is effected as follows.

First, rewrite the constraint as

$$|\underline{D}_T|^2 = |\underline{D}_{TN}|^2 \tag{31}$$

which can be written as

$$\underline{D}_T \cdot \underline{D}_T = \underline{D}_{TN} \cdot \underline{D}_{TN} \tag{32}$$

Let

$$\underline{D}_T = \underline{D}_{TN} + \delta\underline{D}_T \tag{33}$$

Using Equation (33) and neglecting products of perturbations, the left hand side of Equation (32) becomes

$$\underline{D}_T \cdot \underline{D}_T \approx \underline{D}_{TN} \cdot \underline{D}_{TN} + 2\,\underline{D}_{TN} \cdot \delta\underline{D}_T \tag{34}$$

However

$$\delta\underline{D}_T = \underline{D}_T - \underline{D}_{TN} \tag{35}$$

therefore

$$\underline{D}_T \cdot \underline{D}_T \approx 2\,\underline{D}_{TN} \cdot \underline{D}_T - \underline{D}_{TN} \cdot \underline{D}_{TN} \tag{36}$$

Substituting Equation (36) into Equation (32) and rearranging the terms yields the required linear constraint.

$$\underline{D}_{TN} \cdot \underline{D}_{TN} \approx \underline{D}_{TN} \cdot \underline{D}_T \tag{37}$$

4.6 ANGLE OF ATTACK CONSTRAINT

From a re-entry test viewpoint, it is desirable to have the capability to provide near null angle of attack at a specified altitude. This requirement can be fulfilled by the ATHENA vehicle without an active attitude control system on the payload. Due to its simplicity the vehicle cannot always completely null the angle of attack even with perfect system operation. However, the small variations about null that do occur do not compromise the test objectives.

Because the vehicle is spin stabilized the body axis and $\underline{\Delta V}$ (the velocity added by the third and fourth stages) are parallel. Therefore if $\underline{\Delta V}$ and $\frac{d}{dt}\underline{D}_T$ are parallel, the angle of attack will be nulled. From Figure 3 it can be seen that the integral of $\underline{g}$ adds a degree of freedom in the vertical plane that is not present in the horizontal plane. Because there is insufficient freedom in the horizontal plane the impact point and angle of attack constraints can conflict. This conflict is best visualized as follows. It can be seen in Figure 3 that the velocity increment, $\underline{\Delta V}$, will have to be parallel to the vector sum of $\underline{D}_R$ and $\underline{\omega} \times \underline{D}_T$ to null angle of attack in the horizontal plane. In most cases this attitude would not result in a proper impact. Therefore the angle of attack in this plane cannot always be nulled. This problem is not present in the vertical plane because of the extra degree of freedom resulting from the integral of $\underline{g}$.

This restriction does not compromise the usefulness of the system because the deviations from zero angle of attack in the horizontal plane are within acceptable limits. However, the angle of attack constraint equation must be written in a manner that will not result in unrealizable solutions. Therefore, it is necessary to write a constraint equation that causes only the angle of attack in the vertical plane to be nulled. The derivation of this constraint equation follows.

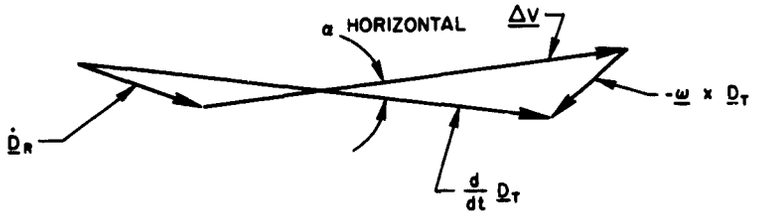

HORIZONTAL PROJECTION

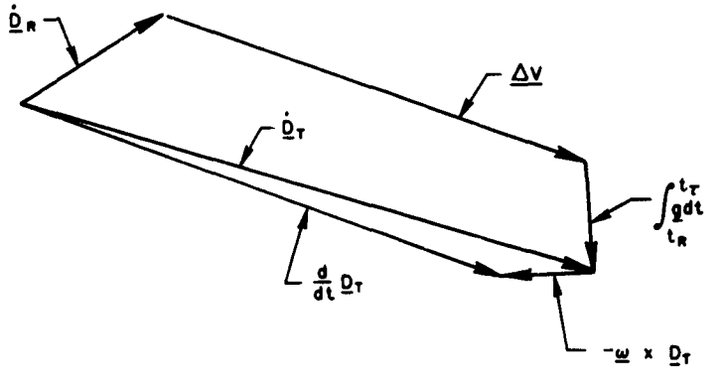

VERTICAL PROJECTION

$$\dot{\underline{D}}_T = \dot{\underline{D}}_R + \Delta\underline{V} + \int_{t_R}^{t_T} \underline{g}\,dt$$

$$\frac{d}{dt}\underline{D}_T = \dot{\underline{D}}_T - \underline{\omega} \times \underline{D}_T$$

Figure 3. Velocity Vector Diagrams

The angle of attack constraint equation is written from inspection of Figure 4. The vector $\underline{\ell}_{TN}$ is normal to the vertical plane defined by $\underline{D}_{TN}$ and $\underline{\Delta V}_N$; that is,

$$\underline{\ell}_{TN} = \underline{D}_{TN} \times \underline{\Delta V}_N \tag{38}$$

Therefore, $\frac{d}{dt}\underline{D}_T \times \underline{\ell}_{TN}$ lies in this vertical plane and is normal to $\frac{d}{dt}\underline{D}_T$.

If

$$\left(\frac{d}{dt}\underline{D}_T \times \underline{\ell}_{TN}\right) \cdot \underline{\Delta V} = 0 \tag{39}$$

then $\underline{\Delta V}$ must lie in the plane shown in Figure 4. Therefore, the projections of $\frac{d}{dt}\underline{D}_T$ and $\underline{\Delta V}$ in the vertical plane must be parallel. This satisfies the angle of attack constraint.

This constraint is linearized as follows. Write Equation (39) in an alternate form.

$$\underline{\ell}_{TN} \cdot \left(\underline{\Delta V} \times \frac{d}{dt}\underline{D}_T\right) = 0 \tag{40}$$

Let

$$\underline{\Delta V} = \underline{\Delta V}_N + \delta\underline{\Delta V} \tag{41}$$

and

$$\frac{d}{dt}\underline{D}_T = \frac{d}{dt}\underline{D}_{TN} + \delta\frac{d}{dt}\underline{D}_T \tag{42}$$

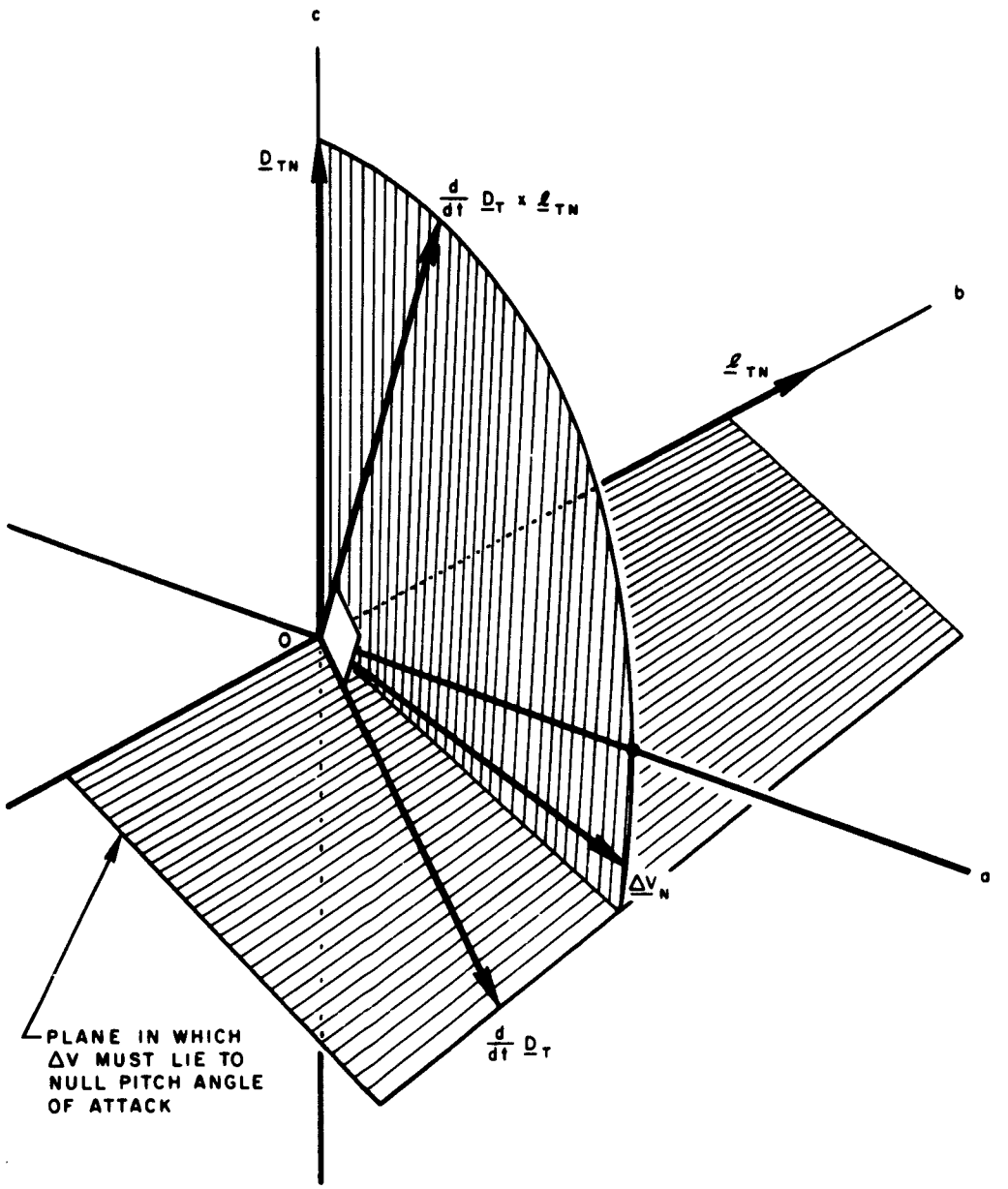

Figure 4. Angle of Attack Geometry

Substituting Equations (41) and (42) into Equation (40), expanding and neglecting products of perturbations yields

$$\frac{d}{dt}\underline{D}_T \cdot (\underline{\ell}_{TN} \times \underline{\Delta V}_N) + \underline{\Delta V} \cdot \left(\frac{d}{dt}\underline{D}_{TN} \times \underline{\ell}_{TN}\right) \approx \underline{\Delta V}_N \cdot \left(\frac{d}{dt}\underline{D}_{TN} \times \underline{\ell}_{TN}\right) \qquad (43)$$

Equation (43) is the linear form of the angle of attack constraint.

4.7 SEPARATION DISTANCE CONSTRAINT

Some of the experiments require a minimum separation distance between the payload and the expended fourth stage at a given altitude. Since the separation velocity increment due to the fourth stage retro rockets is determined before the flight and separation occurs at a fixed time after burnout, the separation distance can be maintained by controlling the time between burnout and arrival at the test altitude.

That is,

$$K_T = t_T - t_\tau \qquad (44)$$

This is the separation distance constraint.

SECTION 5

LINEARIZED EQUATION SUMMARY

The linearized dynamics equations are as follows.

$$\underline{D}_T = \underline{D}_R + \dot{\underline{D}}_R(t_T - t_R) + \underline{\Delta D} + \underline{\Delta V}(t_{TN} - t_{\tau N}) + \underline{\Delta V}_N(t_{\tau N} - t_{TN})$$

$$+ \underline{\Delta V}_N(t_T - t_\tau) + \int_{t_R}^{t_{TN}} \int_{t_R}^{t_1} \underline{g}\, dt\, dt_1 + (t_T - t_{TN}) \int_{t_R}^{t_{TN}} \underline{g}\, dt \qquad (45)$$

$$\underline{D}_I = \underline{D}_R + \dot{\underline{D}}_R(t_I - t_R) + \underline{\Delta D} + \underline{\Delta V}(t_{IN} - t_{\tau N}) + \underline{\Delta V}_N(t_{\tau N} - t_{IN})$$

$$+ \underline{\Delta V}_N(t_I - t_\tau) + \int_{t_R}^{t_{IN}} \int_{t_R}^{t_1} \underline{g}\, dt\, dt_1 + (t_I - t_{IN}) \int_{t_R}^{t_{IN}} \underline{g}\, dt \qquad (46)$$

$$\frac{d}{dt}\underline{D}_T = \dot{\underline{D}}_R + \underline{\Delta V} + \int_{t_R}^{t_{TN}} \underline{g}\, dt - \underline{g}_{TN}(t_{TN} - t_T) - \underline{\omega} \times \underline{D}_T \qquad (47)$$

The direction cosine constraint is

$$1 = (DCx)(DCx_N) + (DCy)(DCy_N) + (DCz)(DCz_N) \qquad (48)$$

The impact point constraint is

$$\underline{D}_I = \underline{E}_{IN} + \underline{\omega} \times \underline{E}_{IN}(t_I - t_{IN}) \qquad (49)$$

The test altitude constraint is

$$\underline{D}_{TN} \cdot \underline{D}_{TN} = \underline{D}_{TN} \cdot \underline{D}_{T} \tag{50}$$

The angle of attack constraint is

$$\frac{d}{dt}\underline{D}_{T} \cdot (\underline{\ell}_{TN} \times \underline{\Delta V}_{N}) + \underline{\Delta V} \cdot (\frac{d}{dt}\underline{D}_{TN} \times \underline{\ell}_{TN}) = \underline{\Delta V}_{N} \cdot (\frac{d}{dt}\underline{D}_{TN} \times \underline{\ell}_{TN}) \tag{51}$$

The separation distance constraint is

$$K_{T} = t_{T} - t_{\tau} \tag{52}$$

SECTION 6

THE ITERATION LOOP, LINEARIZATIONS, AND ACCURACY

There are three types of terms that have been linearized. These are, (1) terms which are functions of body attitude and time, (2) vectors from the center of the earth to the vehicle, and (3) terms which are functions of gravity.

The simple solution of the set of linearized equations will not provide a sufficiently accurate solution for the body attitude and third stage ignition time if the position and velocity at t_R are dispersed from the nominal values by reasonable amounts. This is mainly due to the linearization of the body attitude dependent terms and is overcome with the use of the following iteration procedure.

Because the body attitude (expressed as direction cosines) is determined in the solution of the equations, it is possible to recompute all of the so called "nominal" terms which are functions of body attitude after the solution is complete. Starting with values obtained from the nominal trajectory and recomputing all of the "nominal" terms that are functions of body attitude after the solution of the equations leads to an iterative procedure. This iteration procedure converges on solutions which do not contain errors resulting from the body attitude dependent terms. Perhaps this is more easily understood by examining a particular example. Consider the term $(\underline{\Delta V})\ (t_T)$. The linearization used for this term is

$$(\underline{\Delta V})(t_T) = \underline{\Delta V}(t_{TN}) + \underline{\Delta V}_N(t_T) - \underline{\Delta V}_N(t_{TN}) \tag{53}$$

Because the criterion for convergence is that the direction cosines used to compute the components of $\underline{\Delta V}_N$ are identical to those found from the solution of the equations, the components of $\underline{\Delta V}$ and $\underline{\Delta V}_N$ are equal when the iteration

is completed. Therefore, the first and last terms on the right hand side of Equation (53) cancel and, since $\underline{\Delta V}$ equals $\underline{\Delta V}_N$, the iteration process has nullified errors due to this linearization. Similar reasoning applies to all of the terms which involve body attitude. A diagram of the iteration loop is shown in Figure 5.

Terms containing integrals of $\underline{g}$ have been linearized by expanding them in a Taylor series and retaining only first order terms, with the integrals of $\underline{g}$ considered to be only functions of time. Consequently, the first order position dispersions were disregarded as were the higher order and cross product terms. The adequacy of this assumption has been verified by comparing solutions from the guidance equations with equivalent solutions obtained from a trajectory integration program. It was found that the gravity integral approximations introduce the most significant errors into the guidance equations, but these errors are an order of magnitude smaller than those introduced by other links in the guidance loop (e.g., radar and attitude controller errors) and consequently they can be tolerated.

Because of the nature of the vectors from the center of the earth to the vehicle, the linearization of these vectors does not significantly affect the accuracy of the solution. The solution of the present equations with the iteration on the direction cosines results in an accuracy which easily meets all of the program objectives for the ATHENA missions.

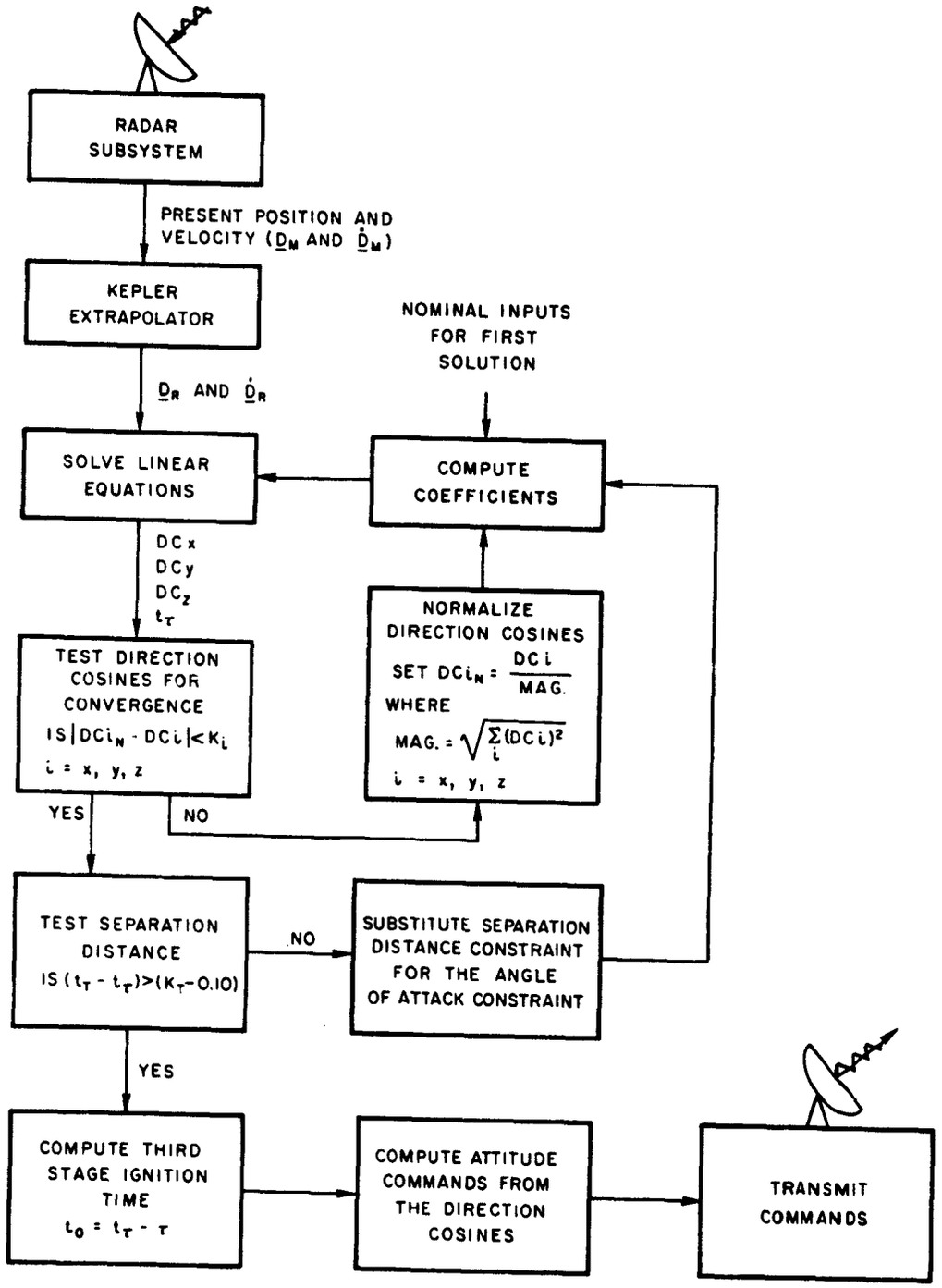

Figure 5. System Block Diagram

REFERENCE

1. Katz, B., Prediction of Position and Velocity by Means of Kepler's Equations, Aerospace Corporation, TOR-269(4810-31)-1, 30 March 1964.

APPENDIX 1

SCALAR EQUATIONS

The expansion of the vector equations in the linearized equation summary to obtain the required scalar equations is presented in this appendix.

The scalar components of Equation (45) are obtained using the expansion of $\underline{\Delta D}$ shown in Equation (19) and a similar expansion for $\underline{\Delta V}$ and $\underline{\Delta V}_N$.

The scalar components are shown in Equation (54) for i = x, y, z.

$$D_{Ti} = D_{Ri} + \dot{D}_{Ri}(t_T - t_R) + |\underline{\Delta D}|DCi + |\underline{\Delta V}|(t_{TN} - t_{\tau N})DCi$$
$$+ |\underline{\Delta V}|(DCi_N)(t_{\tau N} - t_{TN}) + |\underline{\Delta V}|(DCi_N)(t_T - t_\tau)$$
$$+ \int_{t_R}^{t_{TN}} \int_{t_R}^{t_1} g_i dt\, dt_1 + (t_T - t_{TN}) \int_{t_R}^{t_{TN}} g_i dt \qquad (54)$$

Equation (54) can be rewritten in the form

$$A_i = (-1)D_{Ti} + (C_i)t_T + (F_i)DCi + (G_i)t_\tau \qquad (55)$$

where

$$A_i = t_{TN} \int_{t_R}^{t_{TN}} g_i dt - \int_{t_R}^{t_{TN}} \int_{t_R}^{t_1} g_i dt\, dt_1 - D_{Ri} + \dot{D}_{Ri} t_R$$
$$- |\underline{\Delta V}|(DCi_N)(t_{\tau N} - t_{TN}) \qquad (56)$$

$$C_i = |\underline{\Delta V}|(DCi_N) + \dot{D}_{ri} + \int_{t_R}^{t_{TN}} g_i dt \tag{57}$$

$$F_i = |\underline{\Delta D}| + |\underline{\Delta V}|(t_{TN} - t_{\tau N}) \tag{58}$$

$$G_i = -|\underline{\Delta V}|(DCi_N) \tag{59}$$

The scalar components of Equation (46) are obtained in a manner similar to the method used to derive Equation (54) and can be written in the following form, for i = x, y, z.

$$a_i = (-1)D_{Ii} + (e_i)t_I + (f_i)DCi + (h_i)t_\tau \tag{60}$$

where

$$a_i = t_{IN}\int_{t_R}^{t_{IN}} g_i dt - \int_{t_R}^{t_{IN}} \int_{t_R}^{t_1} g_i dt\ dt_1 - D_{Ri} + \dot{D}_{Ri}t_R$$
$$- |\underline{\Delta V}|(DCi_N)(t_{\tau N} - t_{IN}) \tag{61}$$

$$e_i = |\underline{\Delta V}|DCi_N + \dot{D}_{Ri} + \int_{t_R}^{t_{IN}} g_i dt \tag{62}$$

$$f_i = |\underline{\Delta D}| + |\underline{\Delta V}|(t_{IN} - t_{\tau N}) \tag{63}$$

$$h_i = -|\underline{\Delta V}|DCi_N \tag{64}$$

The scalar components of Equation (47) are shown in Equations (65), (66), and (67).

$$\frac{d}{dt} D_{Tx} = \dot{D}_{Rx} + |\underline{\Delta V}| DCx + \int_{t_R}^{t_{TN}} g_x dt - g_{TNx}(t_{TN} - t_T) - \omega_y D_{Tz} + \omega_z D_{Ty} \tag{65}$$

$$\frac{d}{dt} D_{Ty} = \dot{D}_{Ry} + |\underline{\Delta V}| DCy + \int_{t_R}^{t_{TN}} g_y dt - g_{TNy}(t_{TN} - t_T) + \omega_x D_{Tz} - \omega_z D_{Tx} \tag{66}$$

$$\frac{d}{dt} D_{Tz} = \dot{D}_{Rz} + |\underline{\Delta V}| DCz + \int_{t_R}^{t_{TN}} g_z dt - g_{TNz}(t_{TN} - t_T) - \omega_x D_{Ty} + \omega_y D_{Tx} \tag{67}$$

These equations can be written in the following form for i = x, y, z.

$$k_i = (-1)\frac{d}{dt} D_{Ti} + (n_i) DCi + (r_i) t_T + (w_i) D_{Tx} + (s_i) D_{Ty} + (v_i) D_{Tz} \tag{68}$$

where

$$k_i = -\dot{D}_{Ri} - \int_{t_R}^{t_{TN}} g_i dt + g_{TNi} t_{TN} \tag{69}$$

$$n_i = |\underline{\Delta V}| \tag{70}$$

$$r_i = g_{TNi} \tag{71}$$

$$w_x = 0 \quad , \quad w_y = -\omega_z \quad , \quad w_z = +\omega_y \tag{72}$$

$$s_x = +\omega_z \quad , \quad s_y = 0 \quad , \quad s_z = -\omega_x \tag{73}$$

$$v_x = -\omega_y \quad , \quad v_y = +\omega_x \quad , \quad v_z = 0 \tag{74}$$

The scalar components of Equation (49) are shown in Equations (75), (76), and (77).

$$D_{Ix} = E_{INx} + (\omega_y E_{INz} - \omega_z E_{INy})(t_I - t_{IN}) \tag{75}$$

$$D_{Iy} = E_{INy} + (\omega_z E_{INx} - \omega_x E_{INz})(t_I - t_{IN}) \tag{76}$$

$$D_{Iz} = E_{INz} + (\omega_x E_{INy} - \omega_y E_{INx})(t_I - t_{IN}) \tag{77}$$

These equations can be written as follows for i = x, y, z.

$$a_i = (-1)D_{Ii} + (\gamma_i)t_I \tag{78}$$

where

$$a_x = -E_{INx} + (\omega_y E_{INz} - \omega_z E_{INy})t_{IN} \tag{79}$$

$$a_y = -E_{INy} + (\omega_z E_{INx} - \omega_x E_{INz})t_{IN} \tag{80}$$

$$a_z = -E_{INz} + (\omega_x E_{INy} - \omega_y E_{INx})t_{IN} \tag{81}$$

$$\gamma_x = (\omega_y E_{INz} - \omega_z E_{INy}) \tag{82}$$

$$\gamma_y = (\omega_z E_{INx} - \omega_x E_{INz}) \tag{83}$$

$$\gamma_z = (\omega_x E_{INy} - \omega_y E_{INx}) \tag{84}$$

The scalar expansion of Equation (50) is shown below

$$\underline{D}_{TN} \cdot \underline{D}_{TN} = \underline{D}_{TN} \cdot \underline{D}_{T} \tag{85}$$

therefore

$$|\underline{D}_{TN}|^2 = (D_{TNx})D_{Tx} + (D_{TNy})D_{Ty} + (D_{TNz})D_{Tz} \tag{86}$$

The expansion of Equation (51) has the following form

$$(N_x)\frac{d}{dt}D_{Tx} + (N_y)\frac{d}{dt}D_{Ty} + (N_z)\frac{d}{dt}D_{Tz} + (T_x)DCx$$
$$+ (T_y)DCy + (T_z)DCz = W \tag{87}$$

where

$$N_x = \ell_{TNy}|\underline{\Delta V}|DCz_N - \ell_{TNz}|\underline{\Delta V}|DCy_N \tag{88}$$

$$N_y = \ell_{TNz}|\underline{\Delta V}|DCx_N - \ell_{TNx}|\underline{\Delta V}|DCz_N \tag{89}$$

$$N_z = \ell_{TNx}|\underline{\Delta V}|DCy_N - \ell_{TNy}|\underline{\Delta V}|DCx_N \tag{90}$$

$$T_x = (|\underline{\Delta V}|)\left(\ell_{TNz}\frac{d}{dt}D_{TNy} - \ell_{TNy}\frac{d}{dt}D_{TNz}\right) \tag{91}$$

$$T_y = (|\underline{\Delta V}|)\left(\ell_{TNx}\frac{d}{dt}D_{TNz} - \ell_{TNz}\frac{d}{dt}D_{TNx}\right) \tag{92}$$

$$T_z = (|\underline{\Delta V}|)\left(\ell_{TNy}\frac{d}{dt}D_{TNx} - \ell_{TNx}\frac{d}{dt}D_{TNy}\right) \tag{93}$$

$$\begin{aligned} W = {} & |\underline{\Delta V}|DCx_N\left(\ell_{TNz}\frac{d}{dt}D_{TNy} - \ell_{TNy}\frac{d}{dt}D_{TNz}\right) \\ & + |\underline{\Delta V}|DCy_N\left(\ell_{TNx}\frac{d}{dt}D_{TNz} - \ell_{TNz}\frac{d}{dt}D_{TNx}\right) \\ & + |\underline{\Delta V}|DCz_N\left(\ell_{TNy}\frac{d}{dt}D_{TNx} - \ell_{TNx}\frac{d}{dt}D_{TNy}\right) \end{aligned} \tag{94}$$

and

$$\ell_{TNx} = D_{TNy}|\underline{\Delta V}|DCz_N - D_{TNz}|\underline{\Delta V}|DCy_N \tag{95}$$

$$\ell_{TNy} = D_{TNz}|\underline{\Delta V}|DCx_N - D_{TNx}|\underline{\Delta V}|DCz_N \tag{96}$$

$$\ell_{TNz} = D_{TNx}|\underline{\Delta V}|DCy_N - D_{TNy}|\underline{\Delta V}|DCx_N \tag{97}$$

The scalar, linearized equations are presented in matrix form in Equation (98) on the following page. Any symbols that are used in this set of equations that are not defined in the Glossary are defined by equations in this appendix.

$$
\begin{bmatrix} A_x \\ A_y \\ A_z \\ a_x \\ a_y \\ a_z \\ k_x \\ k_y \\ k_z \\ q_x \\ q_y \\ q_z \\ D_{IN}^2 \\ W \\ 1 \end{bmatrix}
\begin{bmatrix}
-1 & 0 & 0 & C_x & 0 & 0 & 0 & 0 & F_x & 0 & 0 & G_x & 0 & 0 & 0 \\
0 & -1 & 0 & C_y & 0 & 0 & 0 & 0 & 0 & F_y & 0 & G_y & 0 & 0 & 0 \\
0 & 0 & -1 & C_z & 0 & 0 & 0 & 0 & 0 & 0 & F_z & G_z & 0 & 0 & 0 \\
0 & 0 & 0 & 0 & -1 & 0 & 0 & e_x & f_x & 0 & 0 & h_x & 0 & 0 & 0 \\
0 & 0 & 0 & 0 & 0 & -1 & 0 & e_y & 0 & f_y & 0 & h_y & 0 & 0 & 0 \\
0 & 0 & 0 & 0 & 0 & 0 & -1 & e_z & 0 & 0 & f_z & h_z & 0 & 0 & 0 \\
0 & s_x & v_x & r_x & 0 & 0 & 0 & 0 & n_x & 0 & 0 & 0 & -1 & 0 & 0 \\
w_y & 0 & v_y & r_y & 0 & 0 & 0 & 0 & 0 & n_y & 0 & 0 & 0 & -1 & 0 \\
w_z & s_z & 0 & r_z & 0 & 0 & 0 & 0 & 0 & 0 & n_z & 0 & 0 & 0 & -1 \\
0 & 0 & 0 & 0 & -1 & 0 & 0 & \lambda_x & 0 & 0 & 0 & 0 & 0 & 0 & 0 \\
0 & 0 & 0 & 0 & 0 & -1 & 0 & \lambda_y & 0 & 0 & 0 & 0 & 0 & 0 & 0 \\
0 & 0 & 0 & 0 & 0 & 0 & -1 & \lambda_z & 0 & 0 & 0 & 0 & 0 & 0 & 0 \\
D_{INx} & D_{INy} & D_{INz} & 0 & 0 & 0 & 0 & 0 & 0 & 0 & 0 & 0 & 0 & 0 & 0 \\
0 & 0 & 0 & 0 & 0 & 0 & 0 & 0 & \Gamma_x & \Gamma_y & \Gamma_z & 0 & N_x & N_y & N_z \\
0 & 0 & 0 & 0 & 0 & 0 & 0 & 0 & DCx_N & DCy_N & DCz_N & 0 & 0 & 0 & 0
\end{bmatrix}
\begin{bmatrix} D_{Tx} \\ D_{Ty} \\ D_{Tz} \\ t_\Gamma \\ D_{Ix} \\ D_{Iy} \\ D_{Iz} \\ t_I \\ DCx \\ DCy \\ DCz \\ t_\tau \\ \frac{d}{dt} D_{Tx} \\ \frac{d}{dt} D_{Ty} \\ \frac{d}{dt} D_{Iz} \end{bmatrix}
\tag{98}
$$

If the earth centered inertial coordinate system is oriented with the z axis aligned with the earth's spin vector $w_z = s_z = v_x = v_y = 0$.

If the separation distance constraint is required, the 14th row of the matrix is replaced by the equation

$$K_T = t_T - t_\tau \tag{99}$$

APPENDIX 2

GLOSSARY

The symbols used in this document are shown graphically in Figures 1 and 2 in addition to being defined in this glossary.

A line under a letter ($\underline{x}$) is used to denote a vector quantity.

A dot above a vector ($\dot{\underline{x}}$) is used to denote the time derivative of the vector relative to an inertial coordinate frame.

Two dots above a vector ($\ddot{\underline{x}}$) are used to denote the second time derivative of the vector relative to an inertial coordinate frame.

The symbol ($\frac{d}{dt}\underline{x}$) is used to denote the time derivative of the vector $\underline{x}$ relative to a rotating coordinate frame.

The first subscript on a vector is used to denote the time at which the vector is expressed.

The subscript N is used to denote nominal parameters. Those nominal parameters which are functions of body attitude are recomputed for each iteration (see Page 25).

$\underline{a}$	=	the thrust acceleration of the vehicle.
$\underline{D}$	=	the vector from the center of the earth to the vehicle.
DCx DCy DCz	=	the three directions cosines of the vehicle body roll axis in the earth centered inertial coordinate system.
$\underline{E}$	=	the vector from the center of the earth to the desired vacuum inpact point.
$\underline{F}$	=	total applied force.
$\underline{g}$	=	the acceleration due to gravity.

$\left.\begin{matrix}\hat{i}\\ \hat{j}\\ \hat{k}\end{matrix}\right\}$	=	orthogonal unit vectors defining the earth centered inertial coordinate system.
K_i	=	convergence constant.
K_T	=	the time between fourth stage burnout and arrival at the test altitude that satisfies the separation distance constraint.
$\underline{\ell}_{TN}$	=	the vector normal to the nominal vertical plane.
m	=	mass.
$\underline{O}$	=	the vector from the desired vacuum impact point to the center of the radar coordinate system.
$\underline{R}$	=	the vector from the radar coordinate system center to the vehicle.
t	=	time (see Figure 2 for specific definitions).
δ	=	the perturbation from the nominal.
$\underline{\Delta D}$	=	the distance travelled during the third and fourth stage thrusting due only to propulsion forces.
$\underline{\Delta V}$	=	the velocity increment due to the third and fourth stage thrusting.
τ	=	the time between third stage ignition and fourth stage burnout.
$\underline{\omega}$	=	the rotation rate of the earth.
t_T	=	time at test altitude.
t_R	=	end point for Keplerian transfer of radar data (chosen as nominal third stage ignition time).
t_0	=	third stage ignition time.
t_τ	=	fourth stage burnout time.
t_I	=	time of impact.
t_M	=	time when adequate radar measurements are available.
t_2	=	second stage burnout time.
t_L	=	launch time.

DISTRIBUTION

Internal

J. R. Allder
G. W. Anderson
J. R. Arnold
F. A. Baskin
R. R. Brown
P. R. Dahl
R. V. Erilane
W. A. Feess
E. Foxman
R. S. Gaylord
A. Gelernter
J. F. Gloudeman
E. A. Goldberg
D. J. Griep
R. Haldin
R. A. Hayes
P. Hines
J. P. Janus
J. J. Jerger
D. G. Kazarian
R. H. Leatherman
J. L. LeMay
J. E. Lesinski
D. MacPherson
R. K. McClean
R. J. McGrath
D. R. McColl
A. S. Mager
H. Marks
J. S. Meditch
D. F. Meronek
R. J. Morra
M. H. Murphy, Jr.
J. C. Peale
W. E. Phillips, Jr.
C. W. Pittman
G. A. Reams
S. Rovell
M. Ruetmann
W. J. Russell
K. A. Sandoval
C. W. Sarture
T. A. Savo
A. J. Schiewe
P. R. Schultz
W. D. Schutt
B. W. Sine
R. V. Soufl
K. F. Steffan
C. H. Tuller
C. R. Welti
J. R. Westlake

DISTRIBUTION (Continued)

External

Defense Documentation Center
Cameron Station
ATTN: TISIA
Alexandria, Virginia (20)

Ballistic System Division
United States Air Force
Norton Air Force Base
California
Capt. D. W. Clonts (BSYA)
Lt. Col. R. H. Parker (BSYA)

Atlantic Research Corporation
Missile Systems Division
Duarte, California
D. Benun
J. D. Knight
J. W. Reed
D. E. Richard

White Sands Missile Range
Data Reduction Division
New Mexico
Maj. Barker
J. Gibson
J. B. Gose
G. L. Pyle

White Sands Missile Range
Flight Simulation Laboratory
New Mexico
G. Hintze
T. Katsura
W. McCool
C. Parker

White Sands Missile Range
Range Operation Directorate
J. Marsh
J. Nance

WSMR, P and P
Capt. B. Neukam